

# Using self-modelling curve resolution for quantification of near infrared spectra of biomedical samples

D. Burns,\* F. Esmonde-White and F. Pandozzi

*McGill University, Montreal H3A 2K6, Canada. E-mail: david.burns@mcgill.ca*

## Introduction

Near infrared spectral measurements of tissue and biofluids are very complex. In biofluids diffuse scattering results in unknown pathlengths through the sample. Likewise, for tissue, when physical structure is added on top of pathlength variations, understanding the relationship of measured spectral response with underlying physiological process is unclear. In general, modelling is difficult since some of the properties are well known while others are not. Self-modelling curve resolution (SMCR) provides a means by which some knowledge of a system can be included, and iterations with the measured data used, to find a self-consistent model of the underlying processes. In the work presented we will show how SMCR can be used to obtain better quantification of underlying constituents in tissue, together with gaining a better understanding of the measurement process. In particular, a method for adaptive modelling of spectra from tissue for myoglobin oxygen saturation will be shown. Likewise, examples of where SMCR can be used to obtain information about a physical process from non-scattering fluids inside a scattering sample are shown.

## Background

Self-Modelling Curve Resolution, also known as Multivariate Curve Resolution is a data analysis tool which seeks to determine the underlying constituents and their concentrations in a mixture from a set of multivariate measurements, where these constituents change concentration. The first description of this technique dates from work of Lawton and Sylvester in the 1970's.<sup>1</sup> During the last 30 years, many refinements of the original work have been made to provide a more robust estimate of the constituents. These techniques have been successfully used for both dual component,<sup>1-3</sup> where unique solutions are possible, as well as multi-component analyses, where solutions are not unique and constraints must be used.<sup>4-8</sup> One member of the SMCR family is alternating least-squares multivariate curve resolution (ALS), based on a series of alternating least squares estimates of composition and spectral components.<sup>6</sup> Constraints are used to isolate the chemical components mathematically, by providing boundaries to limit the possible solutions. Constraints typically used in SMCR algorithms include closure, non-negativity, selectivity, normalisation, and

equality. Spectral data are normally assumed to be non-negative, as are chemical concentrations. However, in tissue spectroscopy, second derivatives are commonly taken as a data pre-treatment step. When derivatives are taken, spectral intensities can assume negative values and non-negativity cannot be used as a constraint. Likewise, concentration closure is no longer applicable when spectral backgrounds are subtracted, because some spectral contribution from each species may be lost. Pre-processing steps must be carefully selected to ensure that constraints chosen for the SMCR remain applicable.

## Materials and methods

In one study, a non-invasive method is developed for analyte quantification in fluids surrounded by optically scattering, opaque walls, such as cerebral spinal fluid behind the skull. To simulate a skull phantom in the laboratory, samples consisted of two distinct layers with details given elsewhere.<sup>9</sup> The first layer had a fixed scattering level, while the second had a variable absorption level. The scattering layer consisted of 1% Intralipid-20 (Fresenius Kabi AB, Uppsala, Sweden) diluted in water, corresponding to a scattering coefficient of approximately  $0.95 \text{ mm}^{-1}$ . Absorbing samples were made by diluting a dye (Dr. Ph. Martin's Juniper Green 12A, Salis International, Hollywood, USA) in water, allowing for a range in absorption coefficient values from 0 to  $0.05 \text{ mm}^{-1}$ . A total of 8 absorbing samples were measured in triplicate. A skull phantom was made

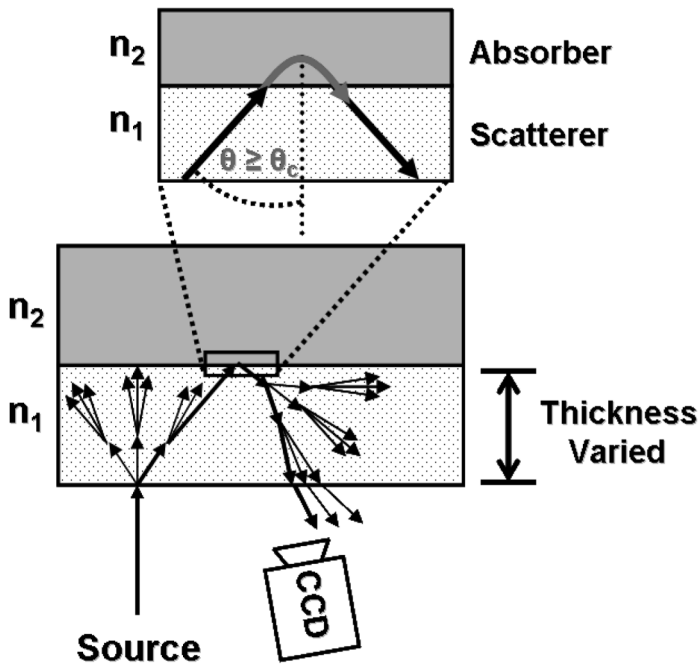


**Figure 1.** Experimental configuration used to study evanescent field effect within a non-scattering sample obscured by a scattering layer of variable thickness.

where the sample cell was divided into two portions: an outer part holding the scattering sample, and an inner compartment holding the absorbing sample. The inner sample cell was attached to a translation stage. This permitted it to be moved forward and backward within the outer sample cell, allowing the thickness of the scattering layer to be easily changed during the experiment. Thicknesses were varied from 1 to 8 mm in steps of 1 mm. Diffuse reflectance measurements were acquired as shown in Figure 1, using one dimension of a  $640 \times 480$  detector array of a Sony XCD-V50 camera (Sony Corp., Japan) having a 14-bit dynamic range.

Signals measured by the detector contain an evanescent field component, which originates from many interactions of the multiply scattered light at the boundary between the scattering and absorbing layer. Examples of the imaging measurements are shown in Figure 2.

The profiles are relatively monotonic, which makes it difficult to discern different contributing components in the data. However, the SMCR approach was used to estimate both analyte concentration and scattering layer thickness between 1 mm and 8 mm of the subsequent images. In a second study, the SMCR technique was compared with a classical least squares method for estimation of myoglobin oxygen saturation in simulated and biological cardiac tissue. Tissue simulations with fixed and variable haemoglobin concentrations were examined to compare the performance of the techniques under different conditions. Likewise, myoglobin oxygen saturation endpoints in 7 guinea pig hearts were estimated from spectra using SMCR and classical

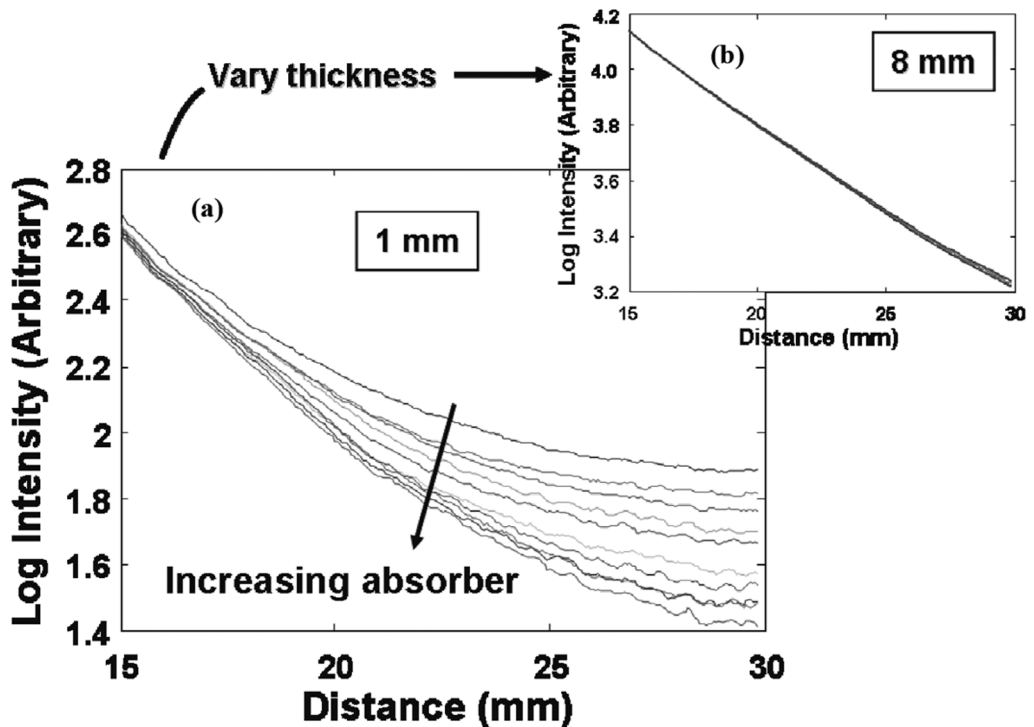


Figure 2. Intensity profiles depicting the effect of absorber variation for scattering layer thicknesses of (a) 1 mm and (b) 8 mm.

least squares (CLS). Spectra of cardiac tissue were collected as previously described in detail.<sup>10,11</sup> Briefly, optical spectroscopic measurements of guinea pig hearts ( $n=7$ ) were recorded between 450 and 950 nm. Excised hearts were perfused with red blood cells at 5% hematocrit under conditions of varying oxygen saturation according to the Langendorff method. Diffuse reflectance spectra were recorded from the left ventricular wall using a custom bifurcated fibre-optic probe having a 1.75 mm separation between source and detector fibres. Spectra were recorded for each excised heart while oxygen saturation of the blood was controlled using a gas-exchange perfusion system to control the oxygen, nitrogen and carbon dioxide concentrations. Maximum myoglobin oxygen saturation was produced experimentally by perfusion with oxygenated buffer, infusion of adenosine to maximally vasodilate the coronary arteries, and infusion of potassium chloride to arrest the heart and thus lower myocardial oxygen consumption. Maximal deoxygenation was produced by infusion of sodium dithionite ( $\text{Na}_2\text{SO}_4$ ) at the end of each experiment.

## Results and discussion

For the first study, systematic variations were observed in signals when both analyte concentration and scatterer thickness were varied for an underlying absorbing fluid behind a scattering layer, as would be consistent with measurements through a skull. Acquired signals were processed using SMCR, which provided both qualitative and quantitative information about the system. Data was shown to be composed of two components using PCA where 99% of the variance is described. For a two component system a unique SMCR estimate of the components is possible. Results of the components are shown in Figure 3.

One component was related to scattering processes in the phantom while another was related to evanescent absorption effects of light trapped within the scattering layer. The first scattering component had a large effect at close source/detector separations, whereas the evanescent component exhibited a peak maximum at larger separations. This information was able to guide further analysis towards regions where maximum signal could be obtained. Diffuse reflectance measurements were also able to provide accurate estimates of scattering layer thicknesses. Likewise, by using the evanescent field effects, good estimation of the absorbing layer hidden behind a highly scattering layer was obtained. In the current configuration, the experimental approach is not complex and can be adapted to a wide range of areas for the analysis of a multitude of samples such as *in-vivo* analyses of cerebrospinal fluid.

In the second study, myoglobin saturation estimates using SMCR with variable haemoglobin composition were shown to decrease estimation error considerably compared to least squares estimates. For simulated tissue spectra results shown in Figure 4, much better estimate myoglobin saturation using SMCR as compared to classical least squares.

Variation about the line of identity for the SMCR estimates are less than 75% of results using classical least squares, even when the endpoint is scaled to a maximum value of 100% saturation. Use of the SMCR method requires that there is measurable variation from each component. In a normally oxygenated heart, the oxygen saturation is approximately 100%. The range of myoglobin saturation required for SMCR to function relative to 100% was examined. Results show that the spectral data set must include myoglobin saturation values that vary from at least 85% to 100% for accurate myoglobin oxygen saturation calibration using SMCR. Exact measurements of intermediate oxygen saturations *in vivo* are difficult; however tissue can be manipulated to achieve

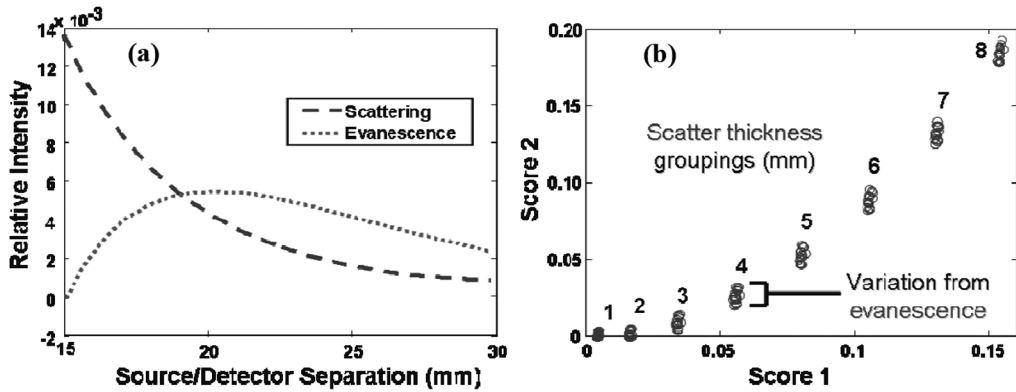


Figure 3. SMCR results showing (a) the scattering and evanescent component profiles and (b) the correlation between the scores associated with these components.

fully saturated (100%) and desaturated (0%) conditions. Results for myoglobin oxygen saturation endpoints in the guinea pig hearts showed saturation estimates using SMCR to be better than estimates using classical least squares. Endpoints at the 100% level were estimated to be 94.3  $\pm$  5.6% using SMCR as compared to 179  $\pm$  27% using classical least squares. Endpoints at 0% oxygen concentration were estimated to be 2.3  $\pm$  1.6% using SMCR as compared to 18  $\pm$  4.3% using classical least squares. SMCR provides a means for practical measurements in clinical settings.

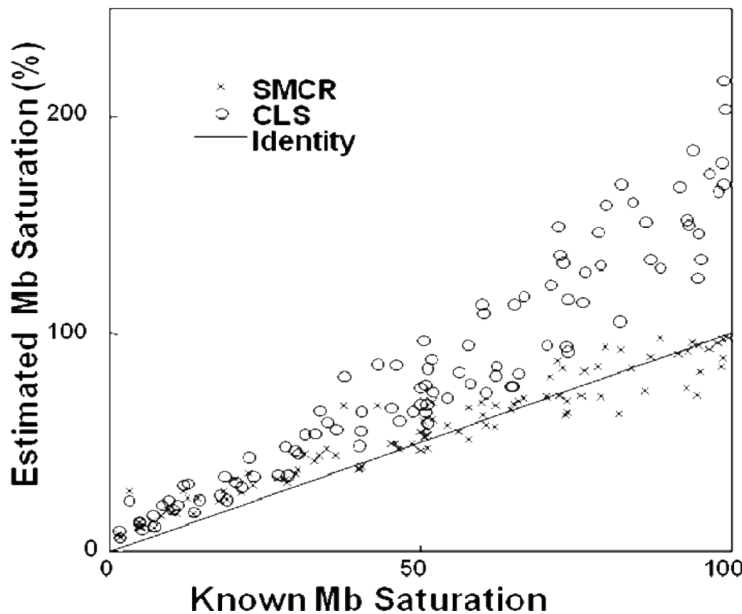


Figure 4. Myoglobin oxygen saturation estimation of tissue phantom spectra using both classical least squares and self modeling curve resolution approach.

## Conclusion

In general, the SMCR approach is a useful tool for analysis of near infrared spectral measurements and provides added insight into the composition and processes of the biomedical problem investigated. As shown in the scattering measurement, sample properties of underlying chromophores can still be estimated at relatively large scattering layer thicknesses. Results suggest that low estimation errors could be achieved when probing tissue samples as thick as 10 mm. Likewise, using spectral measurements, myoglobin oxygen saturation in tissue can be estimated without recording endpoint spectra for calibration. Suitable oxygen saturation ranges should be possible under normal physiological conditions through manipulations of inspired oxygen content. Overall, this work is quite encouraging, and has useful applications in a variety of medical settings.

## References

1. W.H. Lawton and E.A. Sylvestre, *Technometrics* **13**, 617 (1971).
2. T.J. Aartsma, M. Gouterman, C. Jochum, A.L. Kwiram, B.V. Pepich and L.D. Williams, *J. Am. Chem. Soc.* **104**, 6278 (1982).
3. P.J. Gemperline and J.C. Hamilton, *Anal. Chem.* **61**, 2240 (1989).
4. R. Tauler, A. Smilde and B. Kowalski, *J. Chemometr.* **9**, 31 (1995).
5. S. Šaši, Y. Kita, T. Furukawa, M. Watari, H.W. Siesler and Y. Ozaki, *Analyst* **125**, 2315 (2000).
6. S. Navea, R. Tauler and A. de Juan, *Anal. Chem.* **78**, 4768 (2006).
7. J.-H. Jiang, Y. Liang and Y. Ozaki, *Chemometr. Intell. Lab. Syst.* **71**, 1 (2004).
8. T. Azzouz and R. Tauler, *Talanta* **74**, 1201 (2008).
9. F. Pandozzi and D.H. Burns, *J. Near Infrared Spectrosc.* **18**, 17 (2010).
10. K.A. Schenkman, D.R. Marble, E.O. Feigl and D.H. Burns, *Appl. Spectrosc.* **53**, 325 (1999).
11. K.A. Schenkman, D.A. Beard, W.A. Ciesielski and E.O. Feigl, *Am. J. Physiol. Heart Circ. Physiol.* **285**, H1819 (2003).